

# Time-reversal-symmetry-broken quantum spin Hall effect

Yunyou Yang<sup>1</sup>, Zhong Xu<sup>1</sup>, L. Sheng<sup>1,\*</sup>, Baigeng Wang<sup>1</sup>, D. Y. Xing<sup>1,†</sup> and D. N. Sheng<sup>2</sup>

<sup>1</sup>*National Laboratory of Solid State Microstructures and Department of Physics, Nanjing University, Nanjing 210093, China*

<sup>2</sup>*Department of Physics and Astronomy, California State University, Northridge, California 91330, USA*

(Dated: January 15, 2013)

Quantum spin Hall (QSH) state of matter is usually considered to be protected by time-reversal (TR) symmetry. We investigate the fate of the QSH effect in the presence of the Rashba spin-orbit coupling and an exchange field, which break both inversion and TR symmetries. It is found that the QSH state characterized by nonzero spin Chern numbers  $C_{\pm} = \pm 1$  persists when the TR symmetry is broken. A topological phase transition from the TR symmetry-broken QSH phase to a quantum anomalous Hall phase occurs at a critical exchange field, where the bulk band gap just closes. It is also shown that the transition from the TR-symmetry-broken QSH phase to an ordinary insulator state can not happen without closing the band gap.

PACS numbers: 72.25.-b, 73.22.-f, 73.43.-f, 73.20.At

The quantum spin Hall (QSH) effect is a new topologically ordered electronic state, which occurs in insulators without a magnetic field. [1] A QSH state of matter has a bulk energy gap separating the valence and conduction bands, and a pair of gapless spin filtered edge states on the boundary. The currents carried by the edge states are dissipationless due to the protection of time reversal (TR) symmetry and immune to nonmagnetic scattering. The QSH effect was first predicted in two-dimensional (2D) models [2, 3]. It was experimentally confirmed soon after, not in graphene sheets [2] but in mercury telluride (HgTe) quantum wells [3, 4].

Graphene hosts an interesting electronic system. Its conduction and valence bands meet at two inequivalent Dirac points. Kane and Mele proposed that the intrinsic spin-orbit coupling (SOC) would open a small band gap in the bulk and also establish spin filtered edge states that cross inside the band gap, giving rise to the QSH effect [2]. The gapless edge states in the QSH systems persist even when the electron spin  $\hat{s}_z$  conservation is destroyed in the system, e.g., by the Rashba SOC, and are robust against weak electron-electron interactions and disorder [2, 5]. While the SOC strength may be too weak in pure graphene system, the Kane and Mele model captures the essential physics of a class of insulators with nontrivial band topology [6, 7]. A central issue relating to the QSH effect is how to describe the topological nature of the systems. A  $Z_2$  topological index was introduced to classify TR invariant systems [8], and a spin Chern number was also suggested to characterize the topological order [5]. The spin Chern number was originally introduced in finite-size systems by imposing spin-dependent boundary conditions [5]. Recently, based upon the non-commutative theory of Chern number [9], Prodan [10] redefined the spin Chern number in the thermodynamic limit through band projection without using any boundary conditions. It has been shown that the  $Z_2$  invariant and spin Chern number yield equivalent description for TR invariant systems [10–12].

The QSH effect is considered to be closely related to the TR symmetry that provides a protection for the edge states and the  $Z_2$  invariant. An open question is whether or not we can have QSH-like phase in a system where the TR symmetry is broken. Very recently, it was suggested [13] that the quantum anomalous Hall (QAH) effect can be realized in graphene by introducing Rashba SOC and an exchange field. In this Letter, we study the Kane and Mele model by including an exchange field. We calculate the spin Chern number  $C_s$  analytically, and use this integer invariant to distinguish different topological phases in the model with breaking TR symmetry. We find a TR symmetry-broken QSH phase with  $C_{\pm} = \pm 1$ , indicating that the QSH state could survive, regardless of the broken TR symmetry, until the exchange field is beyond a critical value, at which the bulk band gap closes and reopens, and the system enters a QAH phase with  $C_{\pm} = 1$  (or  $-1$ ). By further inclusion of an alternating sublattice potential, we show that the transition from the TR-symmetry-broken QSH phase to an ordinary insulator state is generally accompanied by closing of the band gap. Our conclusion extends the conditions under which the topological QSH state of matter can happen, and opens the door to magnetic manipulation of the QSH effect.

We begin with the Kane and Mele model defined on a 2D honeycomb lattice [2, 5] with the Hamiltonian

$$H = -t \sum_{\langle ij \rangle} c_i^\dagger c_j + \frac{iV_{so}}{\sqrt{3}} \sum_{\langle\langle ij \rangle\rangle} c_i^\dagger \vec{\sigma} \cdot (\vec{d}_{kj} \times \vec{d}_{ik}) c_j + iV_R \sum_{\langle ij \rangle} c_i^\dagger \hat{e}_z \cdot (\vec{\sigma} \times \vec{d}_{ij}) c_j + g \sum_i c_i^\dagger \sigma_z c_i. \quad (1)$$

Here, the first term is the usual nearest neighbor hopping term with  $c_i^\dagger = (c_{i\uparrow}^\dagger, c_{i\downarrow}^\dagger)$  as the electron creation operator on site  $i$  and the angular bracket in  $\langle i, j \rangle$  standing for nearest-neighboring sites. The second term is the intrinsic SOC with coupling strength  $V_{so}$ , where  $\vec{\sigma}$  are the Pauli matrices,  $i$  and  $j$  are two next nearest neighbor

sites,  $k$  is their unique common nearest neighbor, and vector  $\vec{d}_{ik}$  points from  $k$  to  $i$ . The third term stands for the Rashba SOC with coupling strength  $V_R$ , and the last term represents a uniform exchange field of strength  $g$ . For convenience, we will set  $\hbar$ ,  $t$  and the distance between next nearest neighbor sites all to be unity.

We expand Hamiltonian (1) in the long-wavelength limit at Dirac points  $K$  and  $K'$  to the linear order in the relative wave vector  $k = \sqrt{k_x^2 + k_y^2}$  [2]. The base vectors are chosen as  $\{c_{A\uparrow}, c_{A\downarrow}, c_{B\uparrow}, c_{B\downarrow}\}$ , with  $A$  and  $B$  standing for the two sublattices. We consider first the relatively simple case where  $g = 0$  [2]. It is straightforward to find that for  $V_R < V_{so}$ , there is a finite energy gap,  $\Delta_E = \sqrt{3}(V_{so} - V_R)$ , which corresponds to a topological insulating state exhibiting the QSH effect. For  $V_R \geq V_{so}$ , the gap vanishes, and the conduction and valence bands cross at Dirac points  $K$  and  $K'$ . The wave functions for the two valence bands near the Dirac point  $K$  are given by

$$\varphi_{1,2}(\vec{k}) = F_{1,2}(k) \begin{pmatrix} \pm i e^{-2i\theta} \\ \frac{(2E_{1,2} + \sqrt{3}V_{so})e^{-i\theta}}{\sqrt{3}k} \\ \pm \frac{i(2E_{1,2} - \sqrt{3}V_{so})e^{-i\theta}}{\sqrt{3}k} \\ 1 \end{pmatrix}. \quad (2)$$

Here,  $E_{1,2} = \frac{\sqrt{3}}{2}(-\sqrt{k^2 + (V_R \pm V_{so})^2} \pm V_R)$  are the corresponding eigenenergies with subscripts 1 and 2 representing two bands originating from the sublattice degrees of freedom,  $F_1(k)$  and  $F_2(k)$  are normalization constants, and  $\theta$  is the polar angle of  $\vec{k}$  in the reciprocal space.

For finite  $g$ , the obtained analytic expressions for the eigenenergies are too long to write here. The energy gap  $\Delta_E$  between the conduction and valence bands is plotted in Fig. 1a as a function of  $|g|/V_{so}$  for some different values of  $V_R/V_{so}$ . It is found that, for  $V_R < V_{so}$  with increasing  $|g|$  from 0, the gap first decreases; as  $|g|$  reaches a critical value  $g_c$ , the gap closes at  $k = 0$  point; and as  $|g|$  further increases, the gap reopens. The critical exchange energy  $g_c$  is determined by the condition of touching the conduction and valence bands. For  $V_R < V_{so}$ , we have

$$\frac{g_c}{V_{so}} = \frac{\sqrt{3}}{2} \left[ 1 - \left( \frac{V_R}{V_{so}} \right)^2 \right]. \quad (3)$$

It indicates that  $g_c$  decreases with increasing  $V_R/V_{so}$ . For  $V_R \geq V_{so}$ , we have  $g_c = 0$ , and the band gap always exists for finite  $g$ . As will be argued below, the insulating state for  $|g| < g_c$  corresponds to the QSH phase, while that for  $|g| > g_c$  is also topologically nontrivial with gapless chiral edge states, exhibiting a quantized charge Hall conductance.

The definition of spin Chern number  $C_s$  relies on a smooth decomposition of the occupied valence band into two sectors through diagonalization of the electron spin

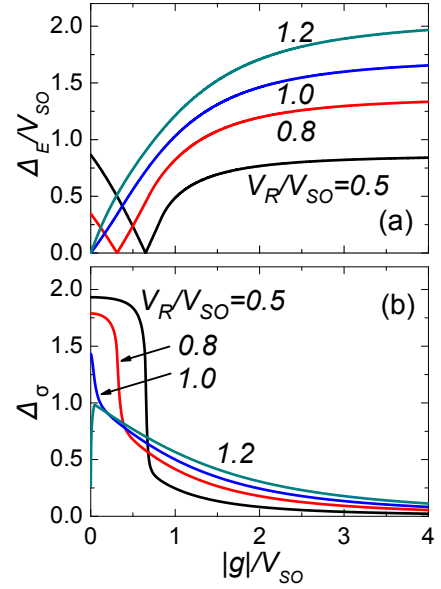


FIG. 1: (a) Normalized energy band gap  $\Delta_E/V_{so}$  and (b) spectrum gap of  $\hat{\sigma}_z$  as functions of  $|g|/V_{so}$  for some different values of  $V_R/V_{so}$ .

operator  $\hat{s}_z = \frac{1}{2}\hat{\sigma}_z$  in the valence band. [10] Since  $\hat{s}_z$  commutes with momentum, the decomposition can be done for each  $\vec{k}$  separately. To simply show the calculation procedure for  $C_s$ , we first discuss the case of  $g = 0$ , where the wave functions  $\varphi_1(\vec{k})$  and  $\varphi_2(\vec{k})$  for the valence band have been given in Eq. (2). By diagonalizing the  $2 \times 2$  matrix  $[\langle \varphi_\alpha(\vec{k}) | \hat{\sigma}_z | \varphi_\beta(\vec{k}) \rangle]$  with  $\alpha, \beta = 1, 2$ , we obtain two eigenfunctions of  $\hat{\sigma}_z$  as

$$\psi_\pm(k) = \frac{1}{\sqrt{2}}[\varphi_1(\vec{k}) \pm \varphi_2(\vec{k})]. \quad (4)$$

The minimal spectrum gap between the eigenvalues of  $\hat{\sigma}_z$  as a function  $|g|/V_{so}$  for different values of  $V_R/V_{so}$ , is plotted in Fig. 1b. The spectrum gap is always nonzero, and so we can unambiguously calculate the corresponding spin Chern numbers [10, 11]. The spin Chern number can be defined as a sum over two Dirac points  $C_\pm = C_{K\pm} + C_{K'\pm}$ , where for the K point [5, 10, 11]

$$C_{K\pm} = \frac{1}{2\pi} \int d^2k Q_{K\pm}(k), \quad (5)$$

with  $Q_{K\pm}(k) = i\hat{e}_z \cdot \langle \nabla_k \psi_\pm(k) | \times | \nabla_k \psi_\pm(k) \rangle$ .  $C_{K'\pm}$  can be defined similarly. By using the polar coordinate system, it is straightforward to obtain  $Q_{K\pm}(k) = \frac{1}{k} \frac{\partial}{\partial k} P_{K\pm}(k)$  with  $P_{K\pm}(k) = \mp 2F_1(k)F_2(k)$ . Substituting the expression for  $Q_{K\pm}(k)$  into Eq. (5), we derive  $C_{K(K')\pm}$  to be

$$C_{K(K')\pm} = [P_{K(K')\pm}(\infty) - P_{K(K')\pm}(0)]. \quad (6)$$

For  $V_R < V_{so}$ , numerical calculation yields  $P_{K(K')\pm}(\infty) = \mp \frac{1}{2}$  and  $P_{K(K')\pm}(0) = \mp 1$ , as shown

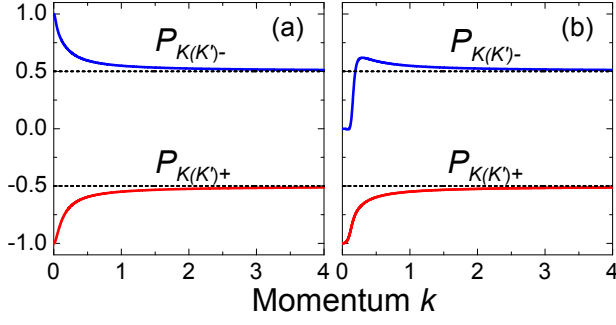


FIG. 2: Calculated  $P_{K(K')\pm}(k)$  for  $V_R/V_{so} = 0.5$ . The exchange energy is taken to be (a)  $g = 0$ , and (b)  $g/V_{so} = 1.2$ .

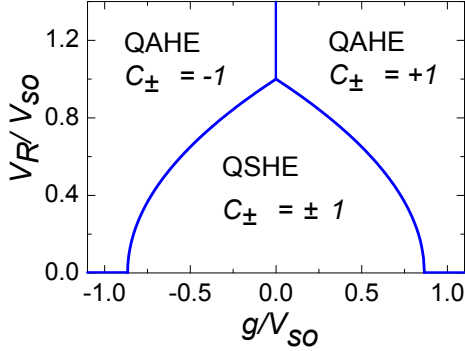


FIG. 3: Phase diagram determined by the Chern numbers in the  $V_R/V_{so}$  versus  $g/V_{so}$  plane. The phase diagram in the half plane of  $V_R/V_{so} < 0$  is mirror symmetric to  $V_R/V_{so} > 0$ , and hence not plotted.

in Fig. 2a. It then follows  $C_{K(K')\pm} = \pm \frac{1}{2}$ , and the total spin Chern numbers are  $C_{\pm} = \pm 1$ . Therefore, at  $g = 0$ ,  $V_R < V_{so}$  corresponds to a topological QSH insulator, as expected.

Now we consider the finite  $g$  case. As has been discussed above, the gaps of energy and spin always exist for finite  $g$  except for  $|g| = g_c$ , so that the spin Chern number can be defined in the whole parameter plane except for  $|g| = g_c$ . Using a procedure similar to that in the  $g = 0$  case outlined above, we obtain  $P_{K\pm}(k)$  and  $P_{K'\pm}(k)$  for both regions  $|g| < g_c$  and  $|g| > g_c$ . It is found that for  $|g| < g_c$ , the curves of  $P_{K(K')\pm}(k)$  are very similar to that in Fig. 2a with  $P_{K(K')\pm}(\infty) = \mp \frac{1}{2}$  and  $P_{K(K')}(0) = \mp 1$  unchanged, yielding  $C_{\pm} = \pm 1$ . Out of this region, we obtain  $C_{\pm} = 1$  for  $g > g_c$  (see Fig. 2b), or  $C_{\pm} = -1$  for  $g < -g_c$ . Figure 3 shows a phase diagram determined by spin Chern numbers in the  $g/V_{so}$  versus  $V_R/V_{so}$  plane. There are three topologically distinct phases characterized by  $C_{\pm} = \pm 1$ ,  $C_+ = C_- = 1$ , and  $C_+ = C_- = -1$ , respectively. From our calculation, the boundary between the different topological phases is just the condition of closing the band gap.

To study the edge states in each region, we calculate the energy spectrum of a long ribbon with zigzag edges

and 240 zigzag chains across the ribbon. For  $|g| < g_c$ , corresponding to  $C_{\pm} = \pm 1$  region in the phase diagram, the energy spectrum is shown in Fig. 4a. One can easily distinguish the edge states from the bulk states. There is a small energy gap in the edge modes as can be seen from the inset of Fig. 4a, due to the absence of TR and inversion symmetries. At a given Fermi level in the band gap, there exist four different edge states labeled as A, B, C, and D. Through the analysis of the spatial distribution of the wave functions, one can find that states A and B localize near one boundary of the ribbon, while C and D localize near the other boundary. Take states A and B on one boundary for example. From the slope of dispersion curves at points A and B, it is easy to determine that the two edge states are counterpropagating. We also examine the spin polarization of the wave functions, state A being almost fully spin-up polarized, and state B spin-down polarized. Therefore, in the  $C_{\pm} = \pm 1$  region there exist two counterpropagating edge states with opposite spin polarizations on a sample edge, which give rise to no net charge transfer but contribute to a net transport of spin.

The characteristic of the edge states in the  $C_{\pm} = \pm 1$  region with  $g \neq 0$  discussed above is very similar to that for the QSH phase at  $g = 0$  protected by the TR symmetry [2]. In particular, they have the same spin Chern number  $C_{\pm} = \pm 1$ , indicating that they belong to the same topological class. As a result, we call it the TR symmetry-broken QSH phase. For the QSH phase protected by the TR symmetry, nonmagnetic impurities do not cause backscattering on each boundary, and the spin transport in the edge states is dissipationless at zero temperature. In the TR symmetry-broken QSH phase, there is usually a weak scattering between forward and backward movers, as evidenced by the small energy gap in the edge state spectrum, leading to a low-dissipation spin transport.

Similar analysis can be applied to the  $C_{\pm} = 1$  region, where the total Chern number of the filled bands sum upto  $C = 2$ , corresponding to a QAH phase [13] with Hall conductivity  $\sigma_{xy} = 2e^2/h$ . The related edge state spectrum is shown in Fig. 4b. It is found that states A and C localize at one boundary and propagate along the same  $-x$  direction, while states B and D localize at the other boundary and propagate along the same  $+x$  direction. As a result, in the QAH phase, two edge states at each boundary lead to spin-up and spin-down currents propagating along the same direction, yielding a quantized charge conductance. The symmetry-broken QSH and QAH phases are topologically distinct. The topological phase transition between them can occur at  $|g| = g_c$  where the band gap just closes.

To further investigate the transition from the TR-symmetry-broken QSH phase to an ordinary insulator state, we include an alternating sublattice potential  $M \sum_{i\tau} \tau c_i^\dagger c_i$  into Hamiltonian (1) with  $\tau = \pm 1$  for  $i$  on sublattice A and B, respectively. For  $g \neq 0$  and  $M \neq 0$ ,

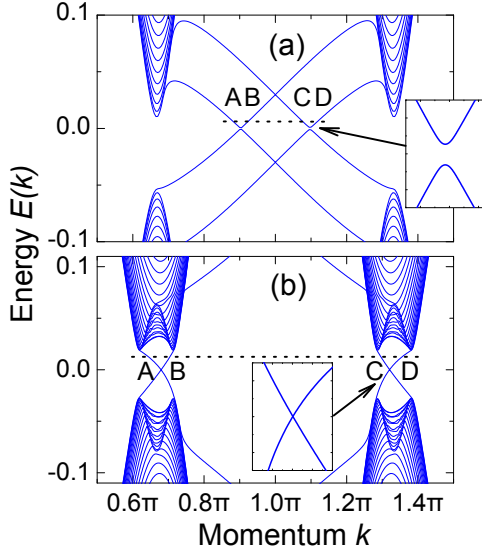


FIG. 4: Energy spectrum of a zigzag-edged graphene ribbon. The parameters are chosen to be  $V_{so} = 0.1$ ,  $V_R = 0.05$ , and  $g = 0.03$  (a) and  $g = 0.15$  (b). At a given Fermi level in the band gap there exist four different edge states, which are labeled as A, B, C, and D.

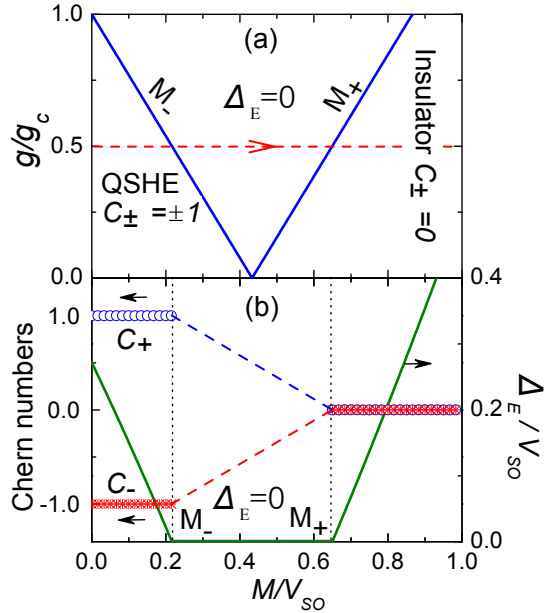


FIG. 5: (a) Phase diagram on the  $g/g_c$  versus  $M/V_{so}$  plane for  $g_c = 0.5 * \frac{\sqrt{3}}{2} V_{so}$ , and (b) calculated Chern numbers and band gap as functions of  $M/V_{so}$  for  $g = 0.5g_c$  and  $V_{so} = 0.1$ .

since both the TR and two-fold rotation symmetries are lifted, the two Dirac cones at  $K$  and  $K'$  become asymmetric, leading to an indirect minimal band gap  $\Delta_E$  between the two Dirac points. We find that for a system initially in the QSH phase of  $|g| < g_c$  with  $g_c$  given by Eq. (3), as  $|M|$  is increased, the indirect band gap closes at a smaller critical value  $|M| = M_-$  and reopens at a

greater critical value  $|M| = M_+$  with  $M_{\mp} = g_c \mp |g|$ . The conduction and valence bands overlap in between, i.e.,  $\Delta_E = 0$  for  $M_- \leq |M| \leq M_+$ . The spin Chern numbers are calculated from the lattice model by projecting the two valence bands into two spin sectors, in a similar manner to that shown above for the continuum model. (For the phase diagram Fig. 3, numerical calculations based upon the lattice model have been performed, the obtained result being found to agree with that from the continuum model.) The spin Chern numbers are well defined only in the regions  $|M| < M_-$  and  $|M| > M_+$ , where  $\Delta_E > 0$ . We find  $C_{\pm} = \pm 1$  for  $|M| < M_-$  and  $C_{\pm} = 0$  for  $|M| > M_+$ . The phase diagram in the  $g$  versus  $M$  plane obtained is plotted in Fig. 5a. The calculated  $C_{\pm}$  and minimal band gap  $\Delta_E$  varying along the arrowed dashed line in Fig. 5a are shown in Fig. 5b as functions of  $M/V_{so}$ . A general feature of the phase diagram is that the transition between the QSH phase with  $C_{\pm} = \pm 1$  and ordinary insulator state with  $C_{\pm} = 0$  is always accompanied by closing of the band gap, which serves as another signature that the TR-symmetry-broken QSH phase is topologically nontrivial and distinct from an ordinary insulator.

This work is supported by the State Key Program for Basic Researches of China under Grants Nos. 2009CB929504, 2007CB925104 (LS), 2011CB922103 and 2010CB923400 (DYX), and the National Natural Science Foundation of China under Grant Nos. 10874066, 11074110 (LS), 11074109 (DYX), and 60825402 (BGW). This work is also supported by the U.S. NSF grants DMR-0906816, DMR-0611562, DMR-0958596 (instrument) and partially by the Princeton MRSEC Grant DMR-0819860 (DNS).

\* Electronic address: shengli@nju.edu.cn

† Electronic address: dyxing@nju.edu.cn

- [1] X.L. Qi and S.C. Zhang, *Physics Today* **63**, 33 (2010).
- [2] C.L. Kane and E.J. Mele, *Phys. Rev. Lett.* **95**, 226801 (2005).
- [3] B.A. Bernevig, T.L. Hughes, and S.C. Zhang, *Science* **314**, 1757 (2006).
- [4] M. Köniig, S. Wiedmann, C. Brune, A. Roth, H. Buhmann, L.W. Molenkamp, X.L. Qi, and S.C. Zhang, *Science* **318**, 766 (2007).
- [5] D.N. Sheng, Z.Y. Weng, L. Sheng, and F.D.M. Haldane, *Phys. Rev. Lett.* **97**, 036808 (2006); L. Sheng, D.N. Sheng, C.S. Ting, and F.D.M. Haldane, *Phys. Rev. Lett.* **95**, 136602 (2005).
- [6] M. Z. Hasan and C. L. Kane, *Rev. Mod. Phys.* **82**, 3045 (2010).
- [7] X. L. Qi and S. C. Zhang, *Rev. Mod. Phys.* (in the press); cond-mat/10122330.
- [8] C.L. Kane, and E.J. Mele, *Phys. Rev. Lett.* **95**, 146802 (2005).
- [9] J. Bellissard, A. van Elst, and H. Schulz-Baldes, *J. Math. Phys.* **35**, 5373 (1994).

- [10] E. Prodan, Phys. Rev. B **80**, 125327 (2009); E. Prodan, New J. Phys. **12**, 065003 (2010).
- [11] H.C. Li, L. Sheng, D.N. Sheng, and D.Y. Xing, Phys. Rev. B **82**, 165104(2010).
- [12] W.-Y. Shan, H.-Z. Lu, S.-Q. Shen, New J. Phys. **12**, 043048 (2010); T. Fukui, and Y. Hatsugai, Phys. Rev. B **75** 121403 (2007); A. M. Essin, and J. E. Moore, Phys. Rev. B **76**, 165307 (2007); B. Zhou, H.-Z. Lu, , R.-L. Chu, S.-Q. Shen, and Q. Niu, Phys. Rev. Lett. **101**, 246807 (2008).
- [13] Z. Qiao, S.A. Yang, W. Feng, W.K. Tse, J. Ding, Y. Yao, J. Wang, and Q. Niu, Phys. Rev. B **82**, 161414(R)(2010).